Materials Science & Engineering A 628 (2015) 230–237

Contents lists available at ScienceDirect

Materials Science & Engineering A

journal homepage: www.elsevier.com/locate/msea

Assessment of the influence of Al–2Nb–2B master alloy on the grain refinement and properties of LM6 (A413) alloy

L. Bolzoni*, M. Nowak, N. Hari Babu

Brunel University London, Institute of Materials and Manufacturing, Brunel Centre for Advanced Solidification Technology, Uxbridge, Middlesex UB8 3PH, UK

ARTICLE INFO

Article history:
Received 16 December 2014
Received in revised form
19 January 2015
Accepted 20 January 2015
Available online 28 January 2015

Keywords:
Al alloys
Grain refinement
Heterogeneous nucleation
Solidification
Nb–B inoculation

ABSTRACT

Cast aluminium alloys are important structural materials but their performances are not optimised due to the lack of appropriate grain refiners. In this study, the effect of the addition of a novel Nb-based grain refiner on the microstructural features and mechanical behaviour of the LM6 alloy (A413) is studied. Specifically, the effect of Nb–B inoculation is assessed over a great range of cooling rates (2–100 °C/s). It is found that Nb-based compounds (i.e., NbB_2 and Al_3Nb) are potent heterogeneous nucleation sites for aluminium and this leads to a significant refinement of the microstructural features. The refinement is not hindered by the formation of silicides, as it happens when using Al–Ti–B master alloys, because niobium silicides form at much higher temperature. It is concluded that the Al–2Nb–2B master alloy is a very effective refiner especially at slow cooling rate and the refinement of the grain size leads to improved performances (homogeneous fine grain structure, mechanical properties and porosity).

1. Introduction

Wrought aluminium alloys are already well-settled materials for the automotive industry where, in the form of sheets, are extensively employed for the production of structural part of the body of the car. Conversely, the application of cast aluminium alloys is not as widely extended as it could be. The main difference between the two types of alloys is the fact that the production of wrought alloys is well optimised, whilst that of cast alloys is not. A very important aspect to be considered for the achievement of optimum formability and mechanical performances is the reduction of the size of the microstructural features such as grain size as well as size and distribution of possible second phases. Different techniques based on treatment of the melt, such as agitation, physical methods (very fast cooling rates that ensure high degree of undercooling), (thermo)-mechanical processes as well as addition of chemical elements, which is known as inoculation, are available. In the former cases, grain refinement (of wrought aluminium alloys) has been obtained though different mechanisms like recrystallization induced by electropulsing as reported by Xu et al. [1], deformation induced precipitation as demonstrated in the work of Cai et al. [2] or by the application high-pressure torsion [3,4]. In the latter case, grain refinement of wrought alloys by inoculation relies on the addition of commercial master alloys based on the Al–Ti–B ternary system [5–10]. The scientific concept behind the grain refinement of wrought aluminium alloys by means of Al–Ti–B master alloys (especially of the Al–5Ti–1B) has been extensively studied [11–16] out of which different mechanisms and theories were proposed such as the one based on "solute", the one which refers to the "peritectic (hulk) reaction", the one developed from "phase diagrams" or the hypernucleation theory, which considered the enhancement of the nucleation on the borides particles from the solutal titanium [5,17,18]. The current understanding about the grain refinement mechanism with Al–Ti–B refiners can be summarised as follows [5–10]: TiB_2 particles act as heterogeneous nucleation sites and Al_3Ti intermetallics dissolve into the molten aluminium providing the needed Ti solute [19]. As per the duplex nucleation theory, a layer of Al_3Ti is formed as transition layer between the surface of the TiB_2 particles and the nucleating aluminium grains. This is due to the fact that Al_3Ti has much favourable lattice match with aluminium than the one between aluminium and TiB_2 intermetallics.

The advantages, improvements, mechanisms and effects as well as drawbacks and challenges of inoculation of Al alloys for their grain refinement are known. The first aspect, which can easily be forgotten, is probably the simplicity of the inoculation process because chemicals are simply added in the molten metal just before casting. The obvious and targeted goal is the promotion of the formation of a great number of grains via heterogeneous nucleation in order to obtain a fine grain size but this also implies that the formation of the typical coarse columnar structure can be easily prevented. Intrinsic advantages of finer microstructural features are not only confined to mechanical properties such as

* Corresponding author. Tel.: +44 1895 267202; fax: +44 1895 269758.
E-mail address: leandro.bolzoni@brunel.ac.uk (L. Bolzoni).

http://dx.doi.org/10.1016/j.msea.2015.01.053

higher yield strength (as per Hall–Petch relationship) and high impact toughness. Actually, technological and manufacturing benefits are really significant among which good formability (for extrusion and rolling processes), good surface finishing, lower propensity to hot tearing and better machinability as a consequence of the more uniform distribution of the second phases and of the shrinkage and gas porosity as well as the soundness of the castings are known. All these benefits are related to the fact that the inoculated melt fills more easily, faster and more efficiently mould cavities as well as allows the melt remaining in between the growing dendritic grains to move more freely enabling the filling of the cavities in the mushy zone of the solidifying metal (i.e., both mass and interdendritic feeding). Among the main concerns and problems relative to the employment of inoculants for the refinement of aluminium and its alloys, it can be named the fact that different manufacturing variables like reaction conditions, ratio of the chemicals, stirring conditions, etc. greatly influence the final refining efficiency. Coarse and agglomerated particles as well as impurities such as salt residues present in the grain refiner generate defect and can cause quality problems. Moreover, the efficiency can be lost by fading, which is either due to the dissolution/interaction of the potential nucleation substrates or the settling (or conversely floating) as a function of the density difference with the molten metal. Finally, impurities coming from the production of the alloy as well as the proper alloying elements have an impact (either enhancing or limiting the grain refining capability) on the refining efficiency and, eventually, can prevent the refinement such as in the case of the poisoning of Ti-based refiners from Zr. As indicated by Quested [20], although grain refinement is beneficial to the casting process, the inoculant particles are seen as unwanted inclusions in downstream processing of ingots.

Because of their high efficiency in refining the grain size of wrought aluminium alloys, it was thought that the addition of Al–Ti–B master alloys to cast aluminium alloys would have the same effect. Nonetheless, from the many studies done it was found that the refinement of cast aluminium alloys, whose main alloying elements is silicon, cannot be efficiently performed by means of Al–Ti–B master alloys. This is due to the fact that silicon reacts with the titanium of the Al–Ti–B master alloys to form titanium silicides (i.e., poisoning [21]) depleting titanium in the melt and, thus, hindering the refinement. Consequently, the development of efficient grain refiner, which allows the production of cast aluminium products with fine equiaxed microstructure instead of coarse columnar grains is of primary significance. Attempts have been made in using other elements rather than titanium because many of them have a relative strong potency (in decreasing order of growth restriction factor: Ti, V, Zr, Nb, Cu, Mg and Si). Furthermore, the effect of the addition of other different alternatives such as variation of the chemical composition of Al–Ti–B master alloys (i.e., Al–3Ti–3B or Al–1Ti–3B), replacement of boron by carbon (i.e., Al–5Ti–0.8C and Al–5Ti–1.2C) and avoidance of titanium (i.e., Al–3B master alloy) has been investigated. We reported the discovery of the application of Nb-based compounds as potent and efficient grain refiners for Al–Si cast alloys where Nb powder and KBF_4 were added to the melt to favour the formation of NbB_2 and Al_3Nb particles [22–24]. Subsequently, a practical way to introduce Nb and B into Al–Si melt was developed in the form of master alloy [25]. The aim of the research reported in this paper is to study the effect of the addition of the Al–Nb–B grain refiners in the form of master alloy to the near-eutectic LM6 alloy (A413 alloy). Specifically, the alloy without and with the addition of the Al–2Nb–2B master alloy is solidified over a large range of cooling rates in order to simulate different industrial processes and its microstructural features analysed. It is worth mentioning that the main features of the LM6 alloy are the excellent castability and dimensional stability as well as good corrosion resistance, good weldability and low specific gravity. As a consequence, this alloy is largely used in two main industrial sectors, specifically the automotive and the marine. In particular, a variety of engine components like connecting rods, pistons, housings, marine fittings and water manifolds are conventionally made out of LM6 alloy processed via casting methods [26]. Furthermore, large-area thin-walled parts with cast-in lettering, intricately designed castings, goods with high-definition details and products where excellent castability, corrosion resistance and pressure tightness (thus ideal for hydraulic cylinders and pressure vessels) are required are typical applications [27]. The high fluidity and possibility to fabricate complex geometries derives by the fact that the LM6 alloy has composition close to that of the eutectic and this permits to obtain also miscellaneous products like architectural panels and spandrels, outdoor lamp housings, lawn mower deck, cooking utensils as well as medical and dental equipment [28].

2. Experimental procedure

The Al–Nb–B master alloy was obtained by mixing commercially pure aluminium (Norton Aluminium, purity $>99.5\%$), with Nb powder (Alfa Aeser, particle size $<45\ \mu m$) and an Al–5B master alloy (LSM). Specifically, the Al–2Nb–2B (weight percent) was targeted. The LM6 alloy (Al–10.5Si–0.3Mg–0.6Fe–0.5Mn–0.1Ni–0.1Zn) was melted into clay bonded graphite crucible at 790 °C during 1 h to homogenise the melt. Afterwards, the reference material (without the addition of any refiner) was left to cool down to 740 °C (± 3 °C) and cast. In the case of the addition of the Al–2Nb–2B master alloy, the level of addition was set to 0.1 wt% equivalent of Nb and the contact time was set to 30 min (which should guarantee the dissolution of the master alloy as well as induce the formation of other Nb-based compounds, whether possible). A 30 mm cylindrical steel mould (cooling rate ~2 °C/s) and a wedge-shaped copper mould (cooling rate range: ~10–1000 °C/s) were used to solidify the alloys. In the case of the cylindrical mould, the microstructural analysis was carried out on the cross-section at 2 cm from the bottom of the samples, whilst the wedge-shape specimens were sectioned into two halves. One side of the samples was ground and macroetched by means of Tucker's solution, whereas the other half was finely polished with OPS for its microstructural analysis. Precisely, the characterisation of the intermetallics was done on polished samples, which were then anodised in order to quantify the grain size of the primary α-Al dendrites. The microstructural analysis was done using a Carl Zeiss Axioskop 2 MAT optical microscope. The linear intercept method was employed for the measurement of the grain size. Thermal analysis, by solidifying the alloys inside a crucible line with glass wool (cooling rate ~0.1 °C/s), was employed to assess the grain refining potency of the Nb–B inoculants considering their effect on the undercooling generated upon solidification. Cooling curves were measured recoding the signal of K-type thermocouples by means of an NI-VI Data Logger (100 data s^{-1}). An Instron® 5569 testing machine was used for the tensile test (ASTM: E8) at a strain rate of $1.33 \times 10^{-3}\ s^{-1}$ of tensile samples machined from bars cast into a permanent mould. The elongation of the samples was recorded by means of an external extensometer (25 mm gauge length). Yield stress values were obtained by means of the offset method.

3. Results and discussion

Fig. 1 shows a SEM micrograph of the cross-section of the Al–2Nb–2B master alloy used to carry out the study.

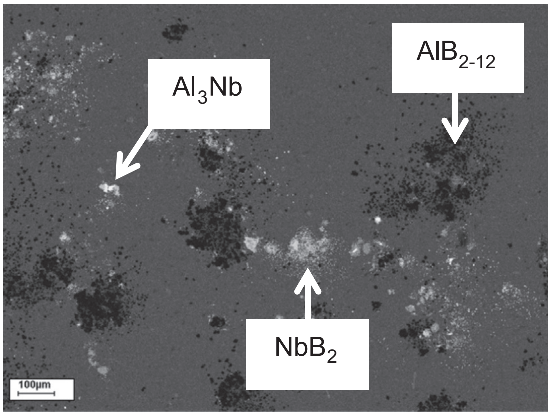

Fig. 1. Micrographs of the Al–2Nb–2B master alloy showing the intermetallic particles found.

From the analysis of the cross-section of the Al–2Nb–2B master alloy, it is found that three different types of intermetallic particles are present. Specifically, aluminium borides (i.e., AlB_2 and AlB_{12}), which derive from the employment of the Al–5B master alloy, and niobium aluminides (i.e., Al_3Nb) and niobium borides (i.e., NbB_2) which originate from the reaction of Nb with Al and B, respectively. The aluminium borides of the Al–5B were formed upon the reaction of molten aluminium with potassium tetrafluoroborate (KBF_4) flux as per:

$$2KBF_4 + 3Al \rightarrow AlB_2 + 2KAlF_4 \quad (1)$$

$$12KBF_4 + 13Al \rightarrow AlB_{12} + 12KAlF_4 \quad (2)$$

The addition of Al–B master alloys and, in particular, of the Al–3B master alloy to Al–Si alloys has been extensively studied [29–31] and it was shown that the presence of these borides as some refining effect in cast Al alloys which, normally, is somewhat better with respect to the Al–Ti–B master alloy such as Al–5Ti–1B [37], Al–3Ti–3B [31,32] and Al–Ti–C refiners [33]. On the basis of our previous study in which the potency of Nb-based compounds was assessed [22–24], both Nb and B alone have some refining effect but nothing comparable to the combined addition of these two elements. Due to the similarities between the Al–Ti–B and the Al–Nb–B ternary systems and the lattice parameters of the compounds that are formed, similar behaviour of the master alloys could be expected. It would be logical to think that, consequently, the Al–Nb–B refiner is characterised by the same poisoning effect by silicon as for the Al–Ti–B master alloy. Nonetheless, this is not the case because the Nb–Si binary phase diagram presents less intermetallics (i.e., niobium silicides), which can be formed [34] and they are stable at much higher temperature [35] in comparison to the titanium silicides of the Al–Ti binary phase diagram [34].

Fig. 2 shows the results of the characterisation performed on the cross-section s of the LM6 alloy samples cast into the cylindrical steel mould.

The comparison of the macroetched cross-sections (Fig. 2a and b) already give a clear impression of the effect of the addition of the Al–2Nb–2B master alloy to the LM6 alloy because the reference material is characterised by quite coarse equiaxed primary dendrites, whilst after addition the size of the dendrites cannot be distinguished easily anymore. A better understanding of the grain size of the dendrites comes from the analysis of the anodised micrographs (Fig. 2c and d) where the grain boundaries of an α-Al dendrites have been highlighted. It can be seen that the grain size of the reference material (Fig. 2c) is in the order of some millimetres, whereas that of the Nb–B refined material (Fig. 2d) is around hundreds of micrometers. By the comparison of the micrographs of the intermetallic phase (Fig. 2e and f), it can be noticed that in the case of the reference the Al–Si eutectic is confined in between the secondary dendritic arms making its distribution quite uneven. After the addition of the Al–2Nb–2B master alloy, the distribution of the eutectic phase is much more uniform throughout the whole microstructure due to smaller grain size. Two types of intermetallic particles are present: Al–Si and Fe-based intermetallics. Concerning the size of these last ones (which have been identified in the micrographs), they are somewhat smaller after the addition of the Al–2Nb–2B master alloy, which is thought to be due to the more homogeneous distribution of the alloying elements in the solidification front and, thus, results in a uniform distribution of finer Fe-based intermetallics in the microstructure. When considering the Al–Si intermetallic phase, it is not easy to claim any variation if not that the reference material comes already with the eutectic phase morphology modified by strontium, which is partially lost after the addition of the Al–2Nb–2B master alloy. This could be due to the mutual poisoning effect of Sr and B but it is most probably due to the loss of Sr by evaporation, which takes place during the re-melting of the virgin alloy.

Figs. 3 and 4 show the summary of the results of the characterisation of the wedge-shaped samples made out of LM6 alloy without and with the addition of the Al–2Nb–2B master alloy, respectively. It is worth mentioning that the cooling rates of the three selected positions are (1) ~5 °C/s, (2) ~15 °C/s and (3) ~100 °C/s.

By the analysis of the microstructural characterisation shown in Fig. 3, it can be seen that the grain size of the primary α-Al dendrites increases with the decrement of the cooling rate employed to solidify the material (i.e., from position 3 to position 1). More in detail, the fast cooling rate at the tip of the wedge-shaped samples leads to quite fine dendrites in the order of hundreds of micron, whilst the slow cooling rate at the wider part of the specimens allows the formation of dendrites of 1–2 mm. Regarding the eutectic phase, as for the case of the cylindrical mould (Fig. 2), it is mainly confined in between the secondary dendritic arms and its size increases with the decreasing of the cooling rate. This same trend can be applied to the size of the Fe-based intermetallics.

From the anodised micrographs of the LM6 alloy after the addition of the Al–2Nb–2B master alloy (Fig. 4), it can be noticed that the material is characterised by very fine equiaxed dendritic grains in the range of 100–400 μm moving from the tip to the wider part of the specimens. Consequently, with respect to the reference material (Fig. 3), the inoculation with Nb-based compounds leads to a significant refinement over a great range of cooling rate making the final grain size less dependent on the extraction of the heat. When considering the eutectic phase, once again this is more uniformly distributed after the addition of the Al–2Nb–2B master alloy. Although the size of the eutectic phase and the Fe-based intermetallics increases for slower cooling rates, this is still relatively finer with respect to the non-refined material.

Fig. 5 shows the comparison of the variation of the grain size versus the cooling rate for the LM6 alloy without and with the addition of the Al–2Nb–2B master alloy.

The trends of the variation of the grain size shown in Fig. 5 are the ones expected on the basis of the discussion of the microstructural analysis. Nonetheless, there are two points that can be stressed from this graph: (1) independently of the employment or not of a grain refiner, the grain size increases exponentially with the decrement of the cooling rate and (2) the grain refining effect of the Nb-based compounds becomes increasingly more important

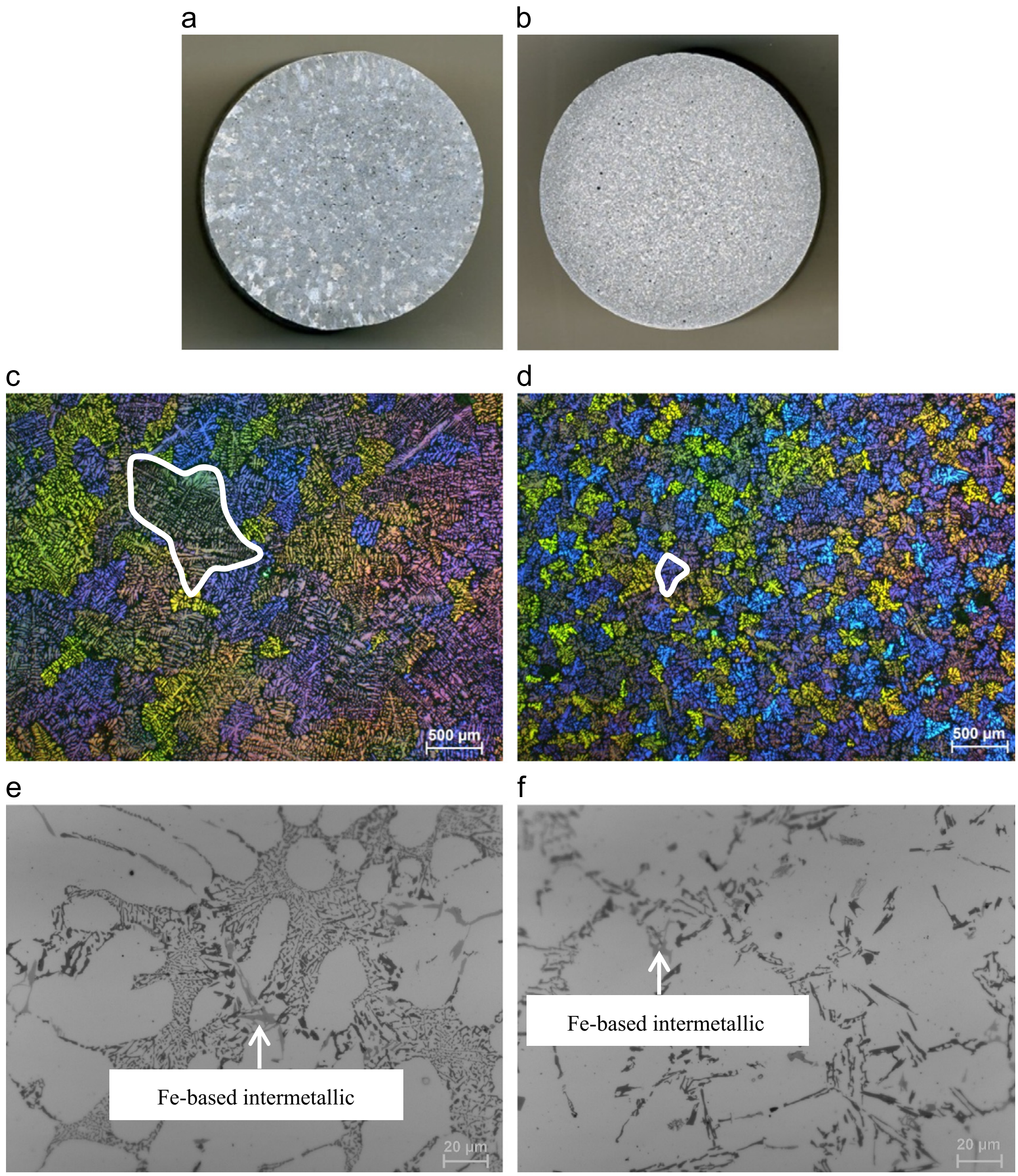

Fig. 2. Results of the LM6 alloy cooled at ~2 °C/s without and with the addition of the Al–2Nb–2B master alloy, respectively: (a) and (b) macroetched cross-sections, (c) and (d) anodised microstructure (the grain boundaries of α-Al dendrites have been highlighted) and (e) and (f) micrograph of the intermetallic phases.

as the material is cooled at slower rate. From the literature, a simplified way to practically represent the variation of the grain size with the cooling rate and quantify the effect grain refiner is [36]

$$d = d_0(dT/dt)^{-n} \tag{3}$$

where d_0 and n (~0.5) are parameters related to the composition of the alloy.

From the inset in Fig. 5, it can be seen that the data relative to the LM6 alloy without and with Nb–B inoculation can be well represented by means of Eq. (3), where $R^2 > 96\%$. The simulation of the variation of the grain size indicates that the effect of Nb–B inoculants during solidification will be vanished at cooling rate of 10^6 (i.e., such as in the case of atomisation processes). Conversely, Nb–B inoculation becomes very important at slow cooling rate in order to obtain fine structures.

The results of the thermal analysis used to estimate the undercooling of the LM6 alloy without and with the addition of the Al–2Nb–2B master alloy are shown in Fig. 6 and Table 1.

Thermal analysis indicates that the reference alloy cools down to 586.0 °C prior to start to form any stable cluster of which can promote the nucleation of primary α-Al grains point from which the temperature increases reaching the coalescence point. The undercooling developed upon the solidification of the reference material is rather high (i.e., 2.7 °C). The introduction of Nb–B inoculants reduces the total undercooling needed during the solidification process down to 0.9 °C. This reduction clearly state that Nb–B inoculants are potent substrate which significantly enhance the heterogeneous nucleation of primary α-Al dendrites because an ideal heterogeneous nucleation site will reduce the undercooling to the lowest possible value [18]. The reduction of the undercooling is also indicating and confirming that the Nb-based inoculants introduced by means of the Al–2Nb–2B master

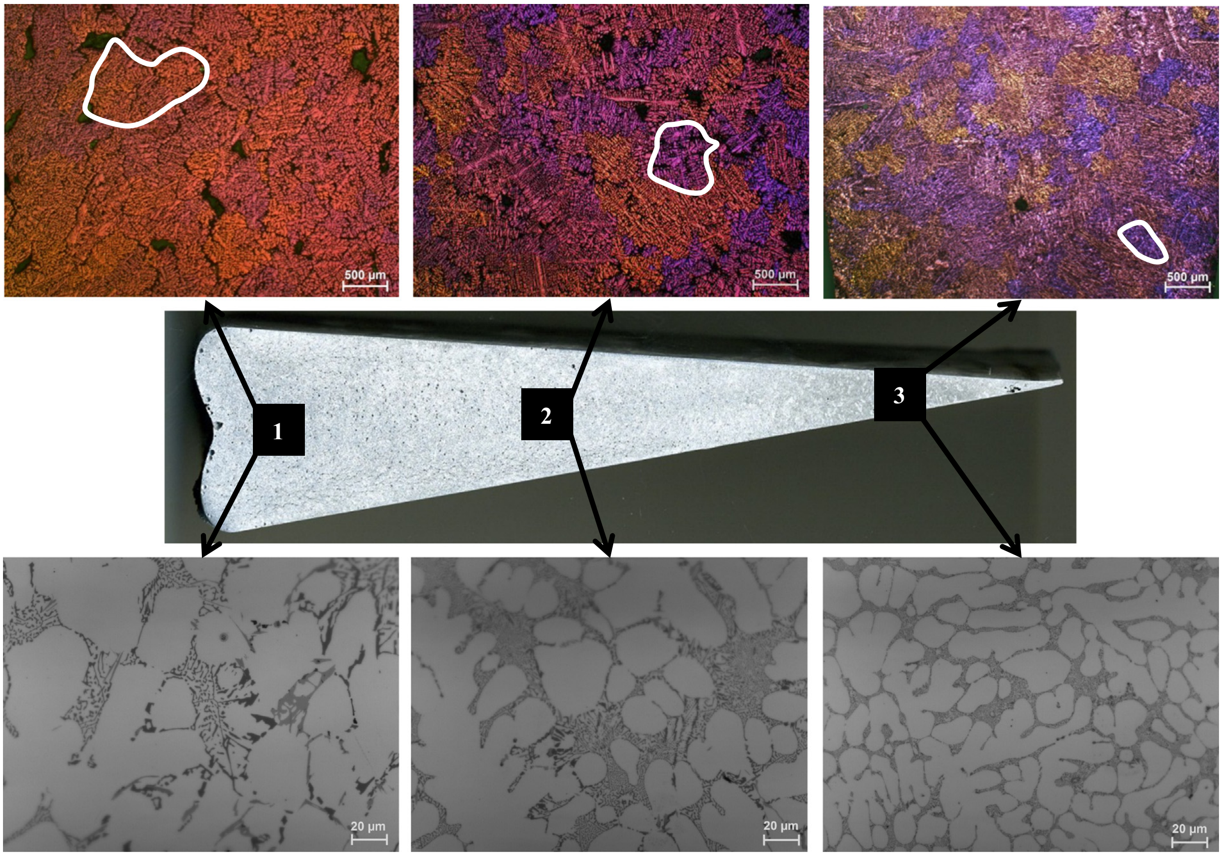

Fig. 3. Summary of the results of the LM6 alloy wedge-shaped samples without the addition of the Al–2Nb–2B master alloy (cooling rates: (1) ~5 °C/s, (2) ~15 °C/s and (3) ~100 °C/s).

alloy have low lattice mismatch with the nucleating phase (i.e., primary α-Al dendritic grains). This is because the undercooling generated for solidification is proportional to the square of the lattice mismatch parameter (f) as found by Turnbull and Vonnegut ($\Delta T \propto f^2$) [37]. That means that the lower the undercooling measured during the thermal analysis the lower the lattice mismatch between the heterogeneous nucleant and the nucleating phase and the more coherent the interphase between these two phases as well as easier to nucleate a proportionally higher number of grains (i.e., grain refinement). The surface of the samples solidified inside the lined crucibles was ground and macroetched (photo not shown for brevity). The grain size estimated from the macroetched cross-sections is in agreement with the one expected from the analysis of the variation of the grain size with the cooling rate (Fig. 5), that is in the order of 3 mm for the reference material and in between 400 μm and 500 μm for the material inoculated with the Al–2Nb–2B master alloy.

The results of the tensile test characterisations (i.e., representative example of the stress–strain engineering curves for LM6 alloy without and with Nb–B inoculation as well as yield and ultimate strength versus elongation) are reported in Fig. 7 [38]. It is worth mentioning that, in the case of the tensile samples, the addition of the grain refiner was done by means of Nb powder and KB_4 flux added directly to the molten alloy. Moreover, for the sake of relating the process with the microstructure and the properties, it is important to indicate that the cooling conditions for these experiments (permanent mould casting) are comparable to those achieved in position 1 in the wedge-shaped samples (see Figs. 3 and 4).

From the representative stress–strain curves, it can be seen that Nb–B inoculation does not change the intrinsic nature of the material because both the LM6 alloy without and with Nb–B addition deforms elastically up to roughly 80 MPa and, afterwards, deforms plastically until reaching the maximum load and fracture. Moreover, the two materials are characterised by similar elasticity (i.e., 71 ± 4 and 75 ± 4 for the material without and with Nb–B addition, respectively) as automatically measured on the stress–strain curves. Nonetheless, Nb–B inoculation leads to an improvement of the mechanical performances of the Al–Si casting alloys both in terms of strength and strain, where the last is most benefited from the much finer primary α-Al grains and finer eutectic grain structure that characterised the microstructure of the Nb–B inoculated alloy. Regarding the strength, the greatest improvement is obtained for the ultimate strength, whereas the increment of the yield stress is rather limited.

As discussed in the introduction, another benefit of the employment of inoculants is the improvement of the soundness of the casting due to the presence of finer pores, whether they are shrinkage and/or gas porosity, as a result of the better feeding and the greater number of growing grains. The effect of Nb–B inoculation, performed by directly adding Nb powder and KB_4 flux to the melt, on the shrinkage porosity and microporosity is presented in Fig. 8.

From the images shown in Fig. 8, it can be seen that, although not quantified, the shrinkage experienced by the alloy during solidification seems to be lower in the case of the inoculation of the material with Nb–B with respect to the reference material. From the inset, where a series of micrographs were taken along the cross-section of the wedge-shaped castings, it can be noticed that the size of the pores is definitively smaller. Concerning the number and distribution of this microporosity, it seems that there are somewhat less pores and they are much more uniformly distributed.

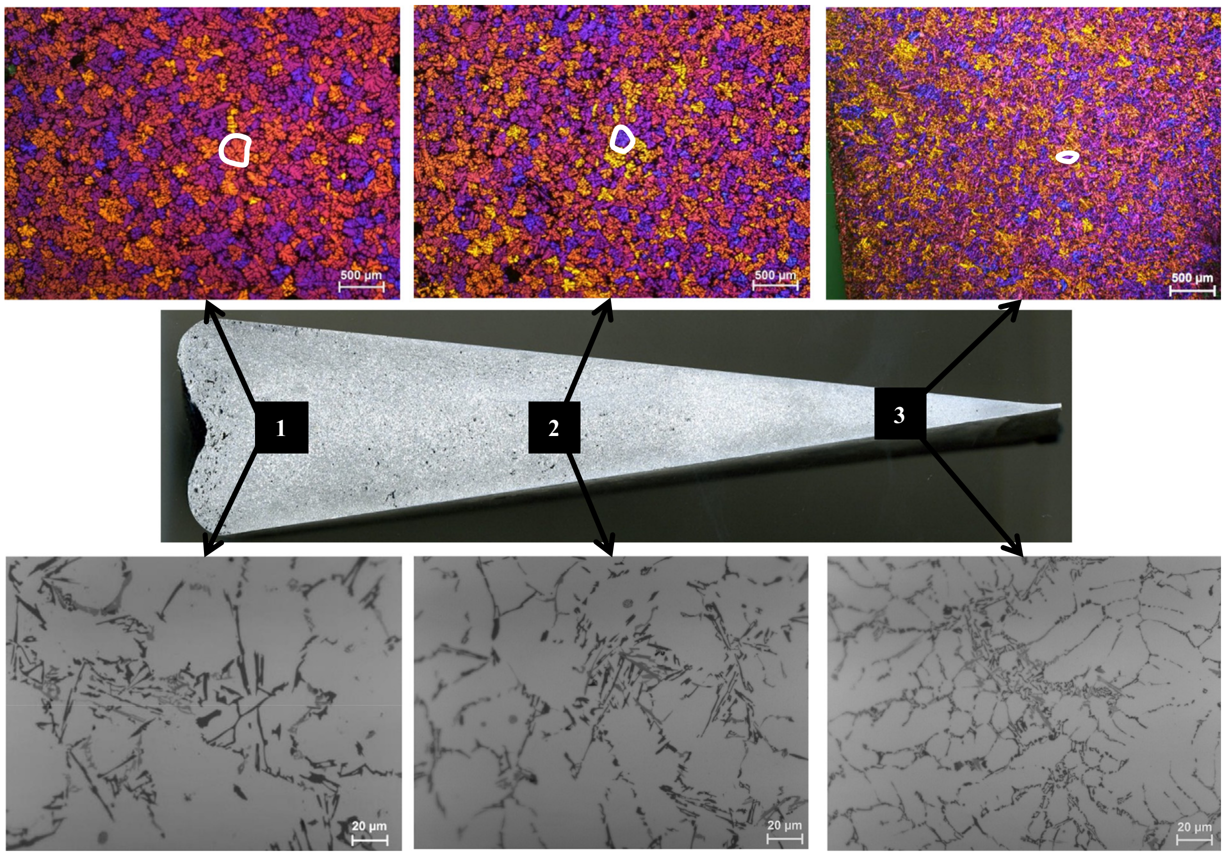

Fig. 4. Summary of the results of the LM6 alloy wedge-shaped samples with the addition of the Al–2Nb–2B master alloy (cooling rates: (1) ~5 °C/s, (2) ~15 °C/s and (3) ~100 °C/s).

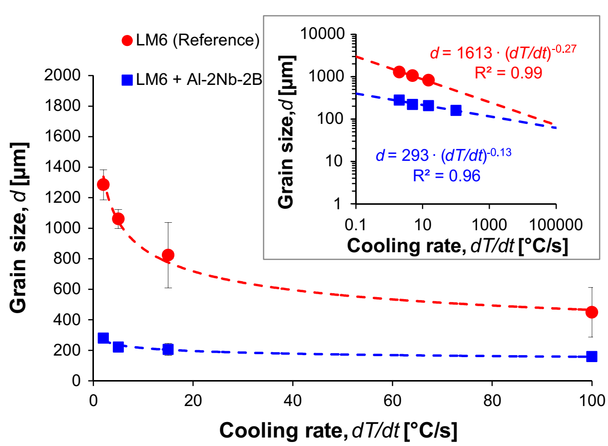

Fig. 5. Variation of the grain size versus the cooling rate for the LM6 alloy without and with the addition of the Al–2Nb–2B master alloy.

The benefits regarding the refinement of the microstructural features, the mechanical properties and the soundness of the casting (i.e., shrinkage and porosity), which are all imputable to better technological performances (such as fluidity and better feeding mechanism) of the inoculated LM6 alloy, are very promising and it is envisaged that they could be applied in aluminium foundries. It is important to stress the fact that Nb–B inoculation permits to obtain primary α-Al dendritic grains over a great range of cooling conditions (see Fig. 5) without much variation of the final grain size depending on the cooling rate. This means that complex and intricate cast structural components characterised by sections with considerable different wall thicknesses will have very similar and comparable grain structure and, thus, mechanical properties. This is not normally the case in cast products because, as it can be evinced from the prediction in Fig. 5, thicker wall-thickness sections will solidify under slower cooling rate (i.e., solidification exclusively controlled by heat extraction) and will have coarse microstructural features in comparison to thin wall-thickness sections. As a consequence of this uneven distribution, the deformation and load withstanding capacity of these sections of a single component are different, which can result in a premature failure of the structural part. Conversely, this also means that generally the engineered components are designed oversize in order to palliate this aspect in order to permit to fulfil the requirement of a minimum safety factor against failure and guarantee that with thicker wall-thickness sections (i.e., coarse grain and, thus, poorer performances) will accomplish the expectation.

An issue, which characterises castings solidified from inoculated aluminium alloy, is that an increase in grain size is observed with the increment of the holding time, which is known as fading of the efficiency of the grain refiner. We reported the fading behaviour of Nb–B inoculants in a previous publication [39] where it was shown that the grain size is still reduced down to approximately 600 µm after 4 h of contact time. The interaction of the chemicals, which compose the grain refiner with the alloying elements of the alloy, can also be a significant issue. It is well known that the efficacy of Al–Ti–B grain refiners in cast Al–Si alloy is poisoned by the formation of titanium silicides. In the case of Nb–B inoculation, no poisoning effect was detected as previously reported [22,23], which is thought to be due to the fact that there are less niobium silicides that can be formed and they are generally at temperature intermetallic compounds. This implies that their kinetics of formation is much slower at the processing temperature of the aluminium industry with respect to those of the titanium silicides. Another important aspect, which is calling a lot of attention, is the recycling of aluminium alloys because the energy costs and emission are much lower compared to

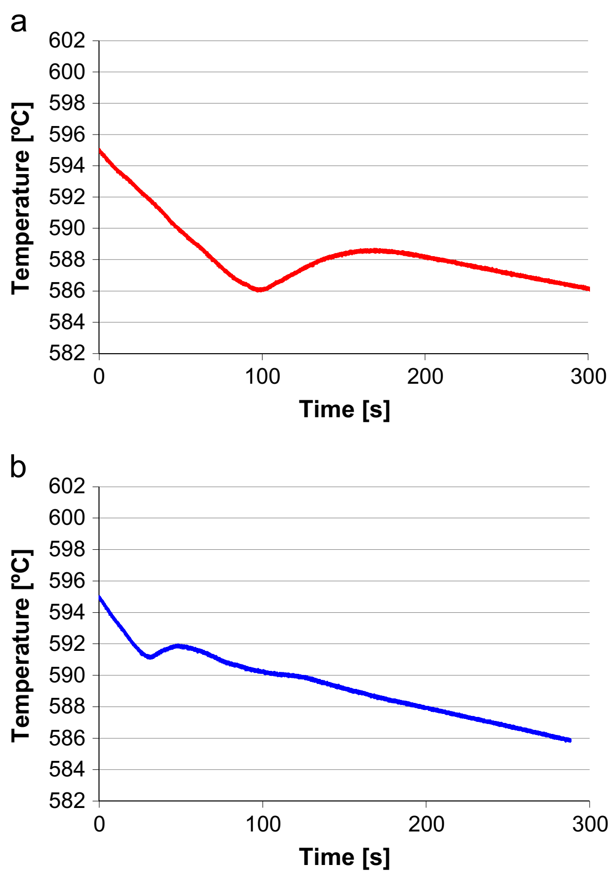

Fig. 6. Cooling curves of the LM6 alloy without (a) and with (b) the addition of the Al–2Nb–2B master alloy.

Table 1
Details of the thermal analysis: T_{min}, $T_{recalescence}$ and ΔT.

Material	Temperature [°C]		Undercooling [°C]
	T_{min}	$T_{recalescence}$	ΔT
Reference	586.0	588.7	2.7
Al–2Nb–2B addition	591.1	592.0	0.9

the extraction of virgin material. Bath analysis is commonly carried out in aluminium foundries and on its base the correct amount of refiner is deemed to be present and/or addition refiner is added [40,41]. This is because the refiners used in most foundries contain both Ti and B and Ti, which is also present, has alloying element or impurities in many cast alloys. We decided to study the recycling of the already inoculated material (Fig. 9) in order to estimate its performance with the number of re-processing steps, that is number of melting and casting after the first inoculation of the material without any further addition of grain refiner.

From Fig. 9, it can be seen that a significant reduction of the grain size is obtained right after the first inoculation of the LM6 alloy and the grain refinement effect is kept up to relatively acceptable level even after three re-processing of the material. Actually, it seems that the most critical step for the recycling of the material is the first re-processing where the grain size increases more noticeable in comparison to the freshly inoculation material. Subsequent re-processing does not seem to further significantly affect the achievable grain size. Out of these experiments it can be stated that the inoculated alloy can be successfully recycled and that the quantity of grain refiner that should be added in order to obtain similar results to the freshly inoculated alloy is predicted to be much lower because the efficacy of Nb–B inoculation is only partly lost during the recycling process.

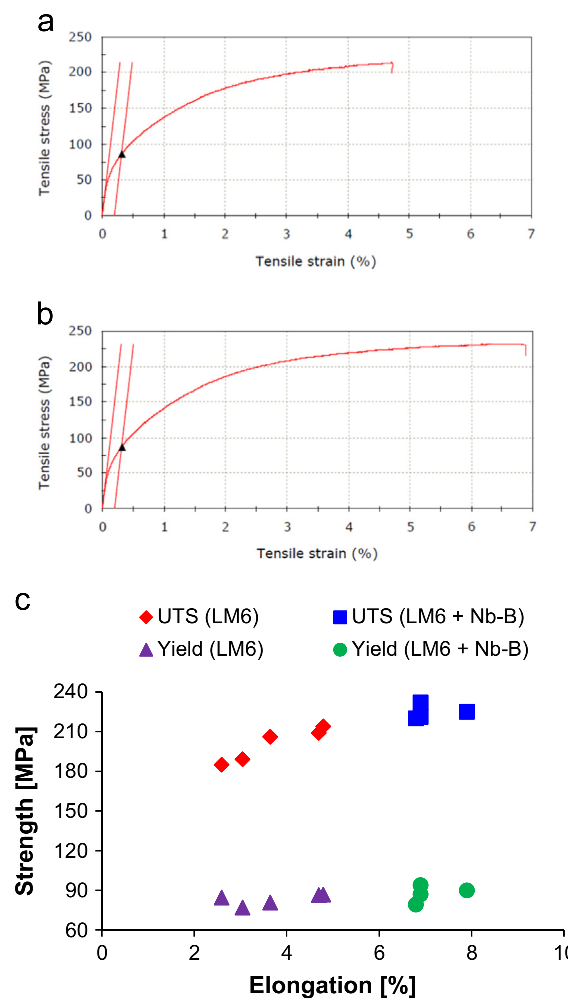

Fig. 7. Representative example of the stress–strain engineering curves for LM6 alloy without (a) and with (b) Nb–B inoculation and (c) yield and ultimate strength versus elongation [38].

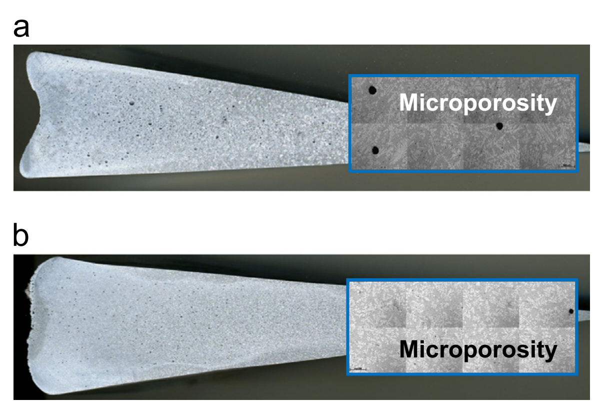

Fig. 8. Representative example of the effect of Nb–B inoculation on the shrinkage and microporosity of the LM6 alloy: (a) reference and (b) Nb–B inoculation [38].

4. Conclusions

From this study about the effect of the addition of a novel Al–2Nb–2B master alloy to the near-eutectic LM6 alloy it can be concluded that Nb-based compounds are highly effective in

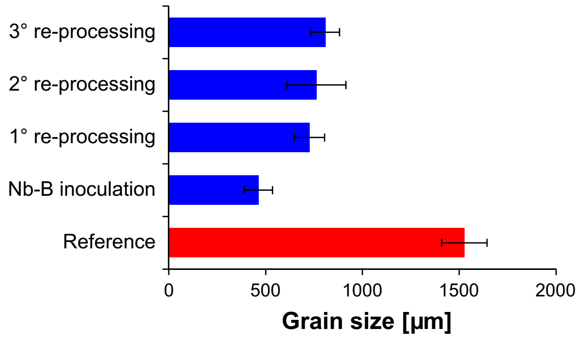

Fig. 9. Results of the re-processing of the Nb–B inoculated LM6 alloy.

refining the primary α-Al dendrites of Al–Si alloys. Moreover, the refinement is kept along a wide range of cooling rate and the greatest difference with respect to the reference materials is seen at slow cooling rate making Nb–B inoculation ideal for sand casting products. The employment of the Al–2Nb–2B master alloy makes the variation of the grain size less dependent on the solidification process (i.e., cooling rate), refines the eutectic phase and permits to obtain a more uniform distribution of the intermetallics, both Si- and Fe-based. The significant grain refinement obtained via Nb–B inoculation results in the improvement performances whether they are mechanical or technological. Specifically, somewhat higher mechanical properties, lower shrinkage and microporosity as well as good recyclability and more independence from the processing parameters (i.e., pouring temperature and cooling conditions) without any visible poisoning are among these performances. From this study, it is envisaged that Nb–B inoculation could be used to produce castings with intricate geometries with more uniform characteristics (grain size, mechanical properties, etc.) or, conversely, used to design lightweight engineered components with thinner sections.

Acknowledgements

The authors are thankful for the financial support from the Technology Strategy Board (TSB) through the TSB/101177 Project and to the Engineering and Physical Sciences Research Council (EPSRC) through the EP/J013749/1 and EP/K031422/1 Projects.

References

[1] X. Xu, Y. Zhao, B. Ma, J. Zhang, M. Zhang, Mater. Sci. Eng. A 612 (2014) 223–226.
[2] Y. Cai, Y. Lang, L. Cao, J. Zhang, Mater. Sci. Eng. A 549 (2012) 100–104.
[3] K. Tugcu, G. Shaa, X.Z. Liao, P. Trimby, J.H. Xia, M.Y. Murashkin, Y. Xie, R.Z. Valiev, S.P. Ringer, Mater. Sci. Eng. A 552 (2012) 415–418.
[4] A. Alhamidi, Z. Horita, Mater. Sci. Eng. A 622 (2015) 139–145.
[5] M. Easton, D.H. St. John, Metall. Mater. Trans. A 30 (1999) 1613–1623.
[6] G.P. Jones, J. Pearson, Metall. Mater. Trans. B 7 (1976) 223–234.
[7] D.H. St. John, L.M. Hogan, J. Aust. Inst. Met. 22 (1977) 160–166.
[8] M.S. Lee, B.S. Terry, Mater. Sci. Technol. 7 (1991) 608–612.
[9] C.D. Mayes, D.G. McCartney, G.J. Tatlock, Mater. Sci. Technol. 9 (1993) 97–103.
[10] A. Hardman, F.H. Hayes, Mater. Sci. Forum 247 (1996) 217–222.
[11] G.K. Sigworth, Metall. Trans. A 15 (1984) 277–282.
[12] G.K. Sigworth, M.M. Guzowski, AFS Trans. 93 (1985) 907–912.
[13] M.M. Guzowski, G.K. Sigworth, D.A. Sentner, Metall. Trans. A 18 (1987) 603–619.
[14] T. Sritharan, H. Li, J. Mater. Process. Technol. 63 (1997) 585–589.
[15] A.L. Greer, P.S. Cooper, M.W. Meredith, W. Schneider, P. Schumacher, J.A. Spittle, A. Tronche, Adv. Eng. Mater. 5 (2003) 81–91.
[16] S. Nafisi, R. Ghomashchi, J. Mater. Process. Technol. 174 (2006) 371–383.
[17] D.G. McCartney, Int. Mater. Rev. 34 (1989) 247–260.
[18] B.S. Murty, S.A. Kori, M. Chakraborty, Int. Mater. Rev. 47 (2002) 3–29.
[19] Y. Birol, J. Alloys Compd. 486 (2009) 219–222.
[20] T.E. Quested, Mater. Sci. Technol. 20 (2004) 1357–1369.
[21] T.E. Quested, A.T. Dinsdale, A.L. Greer, Mater. Sci. Technol. 22 (2006) 1126–1134.
[22] M. Nowak, L. Bolzoni, N. Hari Babu, Mater. Des. 66 (2015) 366–375.
[23] L. Bolzoni, M. Nowak, N. Hari Babu, Mater. Des. 66 (2015) 376–383.
[24] L. Bolzoni, M. Nowak, N. Hari Babu, J. Alloys Compd. 623 (2015) 79–82.
[25] M. Nowak, W.K. Yeoh, L. Bolzoni, N. Hari Babu, Mater. Des. (2015, under review).
[26] T.S. Mahmoudn, S.S. Mohamed, Mater. Sci. Eng. A 558 (2012) 502–509.
[27] J.R. Davis, ASM Speciality Handbook: Aluminum and Aluminum Alloys, ASM International Light Alloys, Ohio, 1993.
[28] J.G. Kaufman, E.L. Rooy, Aluminum Alloy Castings, AFS – American Foundry Society, Ohio, USA, 2004.
[29] Y. Birol, J. Alloys Compd. 513 (2012) 150–153.
[30] Y. Birol, Mater. Sci. Technol. 28 (2012) 385–389.
[31] Y. Birol, Mater. Sci. Technol. 28 (2012) 481–486.
[32] T. Wang, H. Fu, Z. Chen, J. Xu, J. Zhu, F. Cao, T. Li, J. Alloys Compd. 511 (2012) 45–49.
[33] G.S.V. Kumar, B.S. Murty, M. Chakraborty, J. Alloys Compd. 472 (2009) 112–120.
[34] ASM International, ASM Handbook Volume 03: Alloy Phase Diagrams, ASM International, Ohio, 1992.
[35] J.C. Zhao, M.R. Jackson, L.A. Peluso, Mater. Sci. Eng. A 372 (2004) 21–27.
[36] J.A. Dantzig, M. Rappaz, Solidification, EPFL Press, Switzerland (2009) 324.
[37] D. Turnbull, B. Vonnegut, Ind. Eng. Chem. 44 (1952) 1292.
[38] M. Nowak, Development of Niobium–Boron Grain Refiner for Aluminium–Silicon Alloys (Ph.D. thesis), Brunel University, London (UK), 2011 (Available from:).
[39] L. Bolzoni, M. Nowak, N. Hari Babu, Mater Chem Phys (2015, under review).
[40] J.A. Spittle, Foundry Trade J 10 (2008) 308–314.
[41] J.A. Spittle, Foundry Trade J 10 (2008) 335–340.